This article has been accepted for publication in a future issue of this journal, but has not been fully edited. Content may change prior to final publication. Citation information: DOI 10.1109/JSAC.2020.3005494, IEEE Journal on Selected Areas in Communications

Backscatter Aided Wireless Communications on High Speed Rails: Capacity Analysis and Transceiver Design

Wenjing Zhao, Gongpu Wang, Bo Ai, Jian Li, and Chintha Tellambura, *Fellow, IEEE*

***Abstract*—Fast time-varying channel parameters and large penetration losses for signals passing through train carriages are two well-known challenges for wireless communications on high speed rails (HSRs). In this paper, we introduce, for the first time, backscatter technology into HSR wireless communications, which can address these two challenges and yet have low complexity of signal processing and low cost of circuit implementation compared with traditional solutions such as relaying or beamforming. Specifically, we propose a backscatter aided wireless transmission (BAWT) scheme and demonstrate that it outperforms the existing direct wireless transmission (DWT) scheme. We derive the upper and lower bounds of channel capacity for BAWT and prove that it exceeds that of DWT on certain conditions. We also propose the transceiver design for both BAWT and DWT, including joint carrier frequency offset and channel estimator, and signal detector. We show that BAWT, rather than DWT, can obtain the channel statistical information in practical applications due to fixed train antennas and unchanged tracks, which can be utilized to facilitate channel estimation. Finally, simulation results are provided to corroborate the proposed solutions.**

***Index Terms*—Backscatter technology, carrier frequency offset (CFO), channel capacity, channel estimation, high speed rail (HSR), signal detection, wireless communications.**

I. Introduction

Past two decades witness the fast development and deployment of high speed rails (HSRs), especially in China where 35,000 kilometers of HSRs have been built by the end of 2019. Consequently, HSR wireless communications has aroused wide interests from both academic and industrial circles [1] [2].

Unlike other wireless networks, HSR wireless systems are characterized by the high mobility of transceivers and the large penetration loss of the signals passing through train carriages [3]. These two special characteristics give rise to many challenges such as channel modeling, Doppler shift compensation, time-varying channel estimation, fast handover, beamforming and detection [1]. Besides, the applications of the fifth generation wireless technologies on HSRs, i.e., massive multiple-input multiple-output (MIMO) [3] and millimeter wave (mmWave) [4], bring about new open problems for academic research [5].

These challenges of HSR wireless communications have been investigated in a rich body of literature (see [1]–[3], [6] and references therein). The reference [7], for instance, suggests a scheme that estimates a part of the channel through training symbols and reconstructing other parts through spatio-temporal correlation aided by position information. The authors in [8], for another example, investigates Doppler shift estimation problems. The problem of handover on HSRs is studied in [9] where a seamless connectivity scheme is proposed.

A. Motivation

Existing technologies such as full duplex [5], [10], [11], relay [12]–[15], beamforming [16], [17], massive MIMO [18] [19], and joint estimation and detection [20] are possible candidates to reduce or address the signal penetration loss during the transmission between the antennas of base station (BS) and mobile users inside the train. However, these solutions not only require complicated signal processing operations such as demodulation and decoding, but also need radio frequency (RF) components, which are rather expensive.

In this paper, to reduce this signal penetration loss, we introduce another technology, namely backscatter communications. Compared with other existing technologies, backscatter technology has the advantages of low complexity of signal processing and low cost of circuit implementation. Because it avoids demodulation and decoding, and requires no additional RF components [21]–[23]. Specifically, backscattering will not suffer from noise amplifying, which typically exists in amplify-and-forward relays, and has no requirement on signal decoding that is indispensable for decoding-and-forward relay technology. It also avoids the self-interference that full-duplex technology has to face with.

Backscatter communications originated from the second world war and the first paper was published in 1948 by H. Stockman [24]. Backscatter communications are extensively applied for radio frequency identification (RFID) systems. One

Manuscript received December 11, 2019; revised March 16, 2020; accepted April 28, 2020. This study is supported in part by the Natural Science Foundation of China (NSFC) Outstanding Youth under Grant 61725101, in part by NFSC under Grants U1834210, 61871026 and 6196113039, in part by the Royal Society Newton Advanced Fellowship under Grant NA191006, and in part by State Key Lab of Rail Traffic Control and Safety under Grant RCS2020ZT010. (Corresponding author: Gongpu Wang.)

W. Zhao and G. Wang are with Beijing Key Lab of Transportation Data Analysis and Mining, Beijing Jiaotong University, Beijing, China, 100044. Email: {wenjingzhao, gpwang}@bjtu.edu.cn.

B. Ai is with the State Key Laboratory of Rail Traffic Control and Safety, Beijing Jiaotong University, Beijing, China, 100044. Email: boai@bjtu.edu.cn.

J. Li is with the Center for RFIC and System Technology, School of Communication and Information Engineering, University of Electronic Science and Technology of China, Chengdu, China, 611731. Email: lj001@uestc.edu.cn.

C. Tellambura is with the Department of Electrical and Computer Engineering, University of Alberta, Edmonton, AB, CANADA T6G 2V4. Email: chintha@ece.ualberta.ca.

This article has been accepted for publication in a future issue of this journal, but has not been fully edited. Content may change prior to final publication. Citation information: DOI 10.1109/JSAC.2020.3005494, IEEE Journal on Selected Areas in Communications

of the most successful applications of RFID systems is electronic toll Collection that can collect toll fees from vehicles on the high-speedways without stopping them. Backscatter communications have been extensively researched including channel fading and modeling [22], link budgets, multi-antenna techniques [25], and coding methods [23] [26]. To address the rapid development of Internet of Things, researchers have developed several versions backscatter technologies, namely bistatic backscatter [27], ambient backscatter [28] and reconfigurable intelligent surface [29], [30], which enhance coverage and reliability or enable battery-free devices (e.g., sensors or tags) to connect to the Internet [31]. For example, ambient backscatter utilizes ambient RF signals, such as television radio and cellular signals to enable the battery-free tag to communicate with the reader [32]. Backscatter communication is thus becoming a highly active research area [33]–[35].

B. Technical Contributions

It is well-known that high mobility results in large Doppler shifts and hence causes fast time-selectivity in wireless channels, which is quite challenging and even impossible to directly estimate these channels [36]; moreover, future base stations with massive MIMO must estimate a large number channel parameters. However, traditional estimators of time-varying channels compress multiple channel parameters into a few coefficients through basis expansion models (BEMs) [37] [38], auto-regressive models [39] [40], array signal processing models [16], or exploiting channel sparse feature [41] [42]. BEMs decompose the time-varying channel into the superposition of basis functions weighted by time-invariant coefficients. Optimal basis function can be obtained from the channel correlation matrix, which is usually not available in practical situations [6].

Our contributions are summarized as follows:

- By exploiting the low cost and low complexity of backscatter technology, we design a backscatter aided wireless transmission (BAWT) scheme. Specifically, we propose that the train is equipped with two antennas, one outside on the top of the train and the other inside. The outside antenna receives the signals from the BS and the antenna inside amplifies and backscatters the signals to the mobile users inside the train.
- We compare BAWT with direct wireless transmission (DWT) that is currently used in practical HSRs. We derive the upper and lower bounds of channel capacity for BAWT, and prove that on certain conditions, the channel capacity for BAWT is larger than that of DWT.
- We also propose the transceiver design for both BAWT and DWT, including the joint carrier frequency offset (CFO) and time-varying channel estimator and signal detector.

It is worth noting that backscatter technology can also facilitate the estimation of time-varying channels for HSR communication systems. Our proposed BAWT can exploit the channel statistical information that is available in practical applications due to fixed train antennas, which is not applicable for DWT due to the mobility of user terminals.

The rest of the paper is organized as follows. Section II introduces DWT and BAWT schemes and the corresponding mathematical system models. Section III derives and compares the channel capacities between DWT and BAWT. Section IV and V suggest the channel estimator and signal detector for DWT and BAWT schemes, respectively. Section VI provides simulation results to corroborate the proposed studies and Section VII summarizes the whole paper.

Notations: Vectors and matrices are boldface small and capital letters, respectively; the transpose, Hermitian, inverse, and pseudo-inverse of matrix $\mathbf{A}$ are denoted by $\mathbf{A}^T$, $\mathbf{A}^H$, $\mathbf{A}^{-1}$ and $\mathbf{A}^\dagger$, respectively; $\Re\{\mathbf{A}\}$ and $\Im\{\mathbf{A}\}$ are the real and the imaginary part of $\mathbf{A}$, respectively; diag$\{\mathbf{a}\}$ denotes a diagonal matrix with the diagonal elements constructed from $\mathbf{a}$; $\mathrm{E}\{\cdot\}$ denotes the statistical expectation; $\lceil\cdot\rceil$ is the integer ceiling; and the entry indices of vectors and matrices start from 1. $\mathbf{x} \sim \mathcal{CN}(\boldsymbol{\mu}, \boldsymbol{\Sigma})$ denotes that $\mathbf{x}$ is a circularly symmetric complex Gaussian vector with mean $\boldsymbol{\mu}$ and covariance matrix $\boldsymbol{\Sigma}$. The variables with subscript d or b represent relevant ones in the case of DWT or BAWT.

II. System Model

In this system, the BS transmits baseband signals $s(n)$ with the carrier frequency f_{cs} and the initial phase θ_s. Assume that the transmission of $s(n)$ follows a general slotted structure in Fig. 3 [45]. Each slot contains N_p training symbols and N_d data symbols, where $N_p + N_d = N$. There is zero padding, i.e., one or several empty symbols, at the end of each slot to avoid interference between slots or different users. We consider the two transmission schemes: DWT and BAWT.

A. DWT Scheme

Let the direct wireless channel between the BS antenna and that of the mobile user be $h_0(n)$. In DWT, the BS transmits directly to the mobile user through channel $h_0(n)$. Thus, the signal received at the antenna of the mobile user inside the train is expressed as

$$y_d(n) = h_0(n)s(n)e^{j(2\pi f_{cs}n+\theta_s)} + w_0(n),$$

where $w_0(n)$ denotes the additive Gaussian noise at the mobile user. The receiver of the mobile user will then perform a signal down conversion to the baseband. For this task, the receiver will first generate a local carrier signal with carrier frequency f_{cr} and initial phase θ_r. Note that since these two quantities are not identical to f_{cs} and θ_s, this process will introduce a CFO and phase error. Thus, the receiver multiplies $y_d(n)$ with the local carrier to obtain the baseband signal

$$r_d(n) = y_d(n)e^{-j(2\pi f_{cr}n+\theta_r)}. \tag{1}$$

Substituting (1) into (2), we can further rewrite $r_d(n)$ as

$$r_d(n) = h_0(n)s(n)e^{j(2\pi\Delta_f n+\Delta_\theta)} + w(n), \tag{2}$$

where $\Delta_f = f_{cs} - f_{cr}$ is the CFO induced by the down conversion process due to the differences between the crystal oscillators, phase error $\Delta_\theta = \theta_s - \theta_r$, and noise $w(n) = w_0(n)e^{-j(2\pi f_{cr}n+\theta_r)} \sim \mathcal{CN}(0, \sigma_w^2)$.

This article has been accepted for publication in a future issue of this journal, but has not been fully edited. Content may change prior to final publication. Citation information: DOI 10.1109/JSAC.2020.3005494, IEEE Journal on Selected Areas in Communications

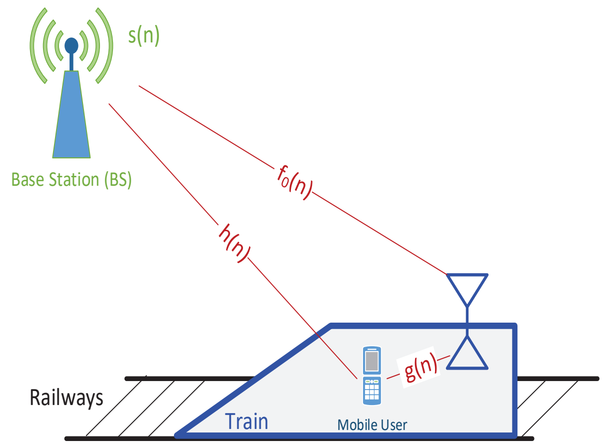

Fig. 1. System model.

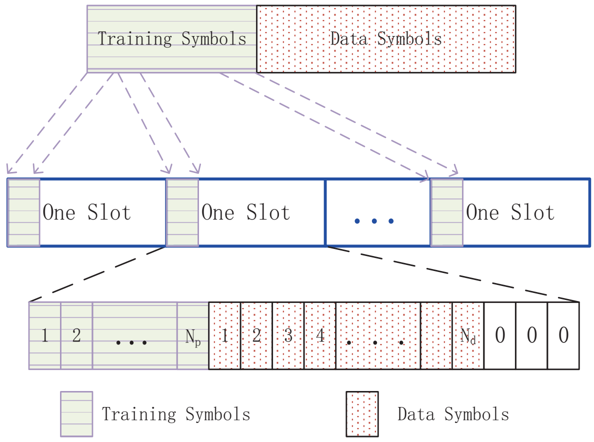

Fig. 3. Transmission slot structure.

Let us define

$$h(n) = h_0(n)e^{j\Delta_\theta} \tag{3}$$

as the combined channel to be estimated. Then, (3) can be rewritten as

$$r_d(n) = e^{j2\pi n\Delta_f} h(n)s(n) + w(n). \tag{4}$$

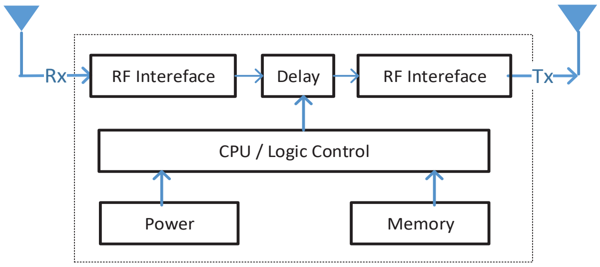

Fig. 2. The block diagram of the backscattering circuit in the train.

B. BAWT scheme

It is worth noting that the carriage penetration loss for HSRs can be as large as 30 dB [10]. To avoid such large loss and to enhance reliability, we propose the BAWT scheme (Fig. 1). It requires the train antenna to first receive the signals from BS and then backscatter them using another antenna inside the train after one symbol duration delay.

Suppose the channel between the antenna of the BS and the outside antenna of the train is $f_0(n)$. The signal received at the train antenna is [1]

$$u(n) = f_0(n)s(n)e^{j(2\pi f_{cs}n+\theta_s)}. \tag{5}$$

BAWT scheme requires that the signal $u(n)$ will be delayed for one symbol duration, and then amplified and backscattered by another antenna inside the train. The corresponding block diagram for the backscattering part is depicted in Fig. 2. The backscattered signal is

$$b(n) = \alpha\eta u(n-1), \tag{6}$$

[1]The Doppler shift is modeled inside the channel $h_0(n)$ and the channel $f_0(n)$, which will be later explained in Section V and Appendix B.

where α is the amplifying coefficient and η denotes the fading inside the two train antennas.

The mobile user will receive both signals from BS directly and from backscattering

$$y_b(n) = h_0(n)s(n)e^{j(2\pi f_{cs}n+\theta_s)} + g(n)b(n) + w_0(n), \tag{7}$$

where $g(n)$ denotes the channel between mobile user and the inside antenna of the train.

Substituting (5) and (6) into (7) yields

$$\begin{aligned} y_b(n) =& h_0(n)s(n)e^{j(2\pi f_{cs}n+\theta_s)} + w_0(n) \\ &+ \alpha\eta g(n)f_0(n-1)s(n-1)e^{j(2\pi f_{cs}(n-1)+\theta_s)}. \end{aligned}$$

The mobile user will generate a carrier signal to demodulate $y_b(n)$ and will obtain

$$\begin{aligned} r_b(n) =& y_b(n)e^{-j(2\pi f_{cr}n+\theta_r)} \\ =& h_0(n)s(n)e^{j(2\pi\Delta_f n+\Delta_\theta)} + w(n) \\ &+ \alpha\eta g(n)f_0(n-1)s(n-1)e^{j2\pi\Delta_f n}e^{j\Delta_\theta}e^{-j2\pi f_{cs}}. \end{aligned} \tag{8}$$

We note that the channel $g(n)$ remains almost unchanged during several time slots due to the limited mobility of the mobile user inside the train. Therefore, it is reasonable to approximate $g(n)$ as a slow-fading random variable g_0 within one slot. We thus assume $g_0 \sim \mathcal{CN}(0, \sigma_{g0}^2)$.

Let us denote the composite channel to be estimated as

$$f(n-1) = \alpha\eta g_0 f_0(n-1)e^{-j2\pi f_{cs}}e^{j\Delta_\theta}. \tag{9}$$

The signal $r_b(n)$ can be simplified as

$$\begin{aligned} r_b(n) =& e^{j2\pi n\Delta_f}h(n)s(n) \\ &+ e^{j2\pi n\Delta_f}f(n-1)s(n-1) + w(n). \end{aligned} \tag{10}$$

C. Transmission Goals

Let $\mathcal{T}_p$ and $\mathcal{T}_d$ be the time index set for the training symbols and information symbols respectively. Clearly, the cardinality of the set should be $|\mathcal{T}_p| = N_p$ and $|\mathcal{T}_d| = N_d$. Without loss of generality, we assume that $\mathcal{T}_p = [p_1, p_2, \cdots, p_{N_p}]$ and $\mathcal{T}_d = [d_1, d_2, \cdots, d_{N_d}]$.

This article has been accepted for publication in a future issue of this journal, but has not been fully edited. Content may change prior to final publication. Citation information: DOI 10.1109/JSAC.2020.3005494, IEEE Journal on Selected Areas in Communications

The goal for DWT is to first estimate the CFO Δ_f and the channel $h(n)$ using the training symbols $s(n), n \in \mathcal{T}_p$, and then recover the discrete information signal $s(n), n \in \mathcal{T}_d$ in (4), while BAWT aims to obtain estimates of not only Δ_f and $h(n)$, but also $f(n)$ in (10), and next recover $s(n), n \in \mathcal{T}_d$, which will be addressed in the following two sections.

Remark 1. *Both CFO and Doppler shift resulted from train speed can lead to time selectivity in wireless channels. It is worth noting that our proposed system models of DWT and BAWT consider the CFO and the Doppler shift separately. That is, the CFO Δ_f appears in the received signals while the Doppler shift is hidden in channels $h(n)$ and $f(n)$. We separate them intentionally so as to facilitate channel estimation, which will be discussed in Section V.*

III. Capacity Analysis

For brevity of our analysis, let us define the transmitted signals $s(n)$ and the channels $h(n)$ and $f(n)$ in one slot as $\mathbf{s} = [s(1), s(2), \cdots, s(N)]^T$, $\mathbf{h} = [h(1), h(2), \cdots, h(N)]^T$ and $\mathbf{f} = [f(1), h(2), \cdots, f(N)]^T$, respectively. In the case of DWT, define the corresponding received signal vector $\mathbf{r}_d$ and the noise vector $\mathbf{w}_d$ as $\mathbf{r}_d = [r_d(1), r_d(2), \cdots, r_d(N)]^T$ and $\mathbf{w}_d = [w(1), w(2), \cdots, w(N)]^T$, respectively; in the case of BAWT, the corresponding received signal vector $\mathbf{r}_b$ and the noise vector $\mathbf{w}_b$ are separately denoted by $\mathbf{r}_b = [r_b(1), r_b(2), \cdots, r_b(N), r_b(N+1)]^T$ and $\mathbf{w}_b = [w(1), w(2), \cdots, w(N), w(N+1)]^T$. Define $\mathbf{S} = \mathrm{diag}\{\mathbf{s}\}$, $\mathbf{H} = \mathrm{diag}\{\mathbf{h}\}$ and $\mathbf{F} = \mathrm{diag}\{\mathbf{f}\}$. Herein, we assume that the equivalent channels $h(n)$ and $f(n)$ are distributed as $h(n) \sim \mathcal{CN}(0, \sigma_h^2)$ and $f(n) \sim \mathcal{CN}(0, \sigma_f^2)$, respectively.

A. DWT

We can rewrite (4) as

$$\mathbf{r}_d = \mathbf{D}_d(\Delta_f)\mathbf{H}\mathbf{s} + \mathbf{w}_d, \tag{11}$$

where

$$\mathbf{D}_d(\Delta_f) = \mathrm{diag}\{e^{j2\pi\Delta_f}, e^{j4\pi\Delta_f}, \cdots, e^{j2\pi N\Delta_f}\}.$$

If the receiver knows the channel state information (CSI), the capacity of (11) is equal to

$$\begin{aligned} C_d =& \frac{1}{N}\mathrm{E}\left\{\log\det(\mathbf{I} + \gamma\mathbf{D}_\mathrm{d}(\Delta_\mathrm{f})\mathbf{H}\mathbf{H}^\mathrm{H}\mathbf{D}_\mathrm{d}^\mathrm{H}(\Delta_\mathrm{f}))\right\} \\ =& \frac{1}{N}\sum_{n=1}^{N}\mathrm{E}\left\{\log(1+\gamma|\mathrm{h(n)}|^2)\right\}, \end{aligned} \tag{12}$$

where γ stands for singal-to-noise ratio (SNR).

It can be readily checked that the probability density function of $|h(n)|^2$ is $f_{h^2}(x) = \frac{1}{\sigma_h^2}\exp\left(-\frac{x}{\sigma_h^2}\right)$ [43]. Then, with the aid of [44, eq. (4.337)], (12) can be derived as

$$C_d = -\exp\left(\frac{1}{\gamma\sigma_h^2}\right)\mathrm{Ei}\left(-\frac{1}{\gamma\sigma_h^2}\right), \tag{13}$$

where $\mathrm{Ei}(x) = \int_{-\infty}^{x}\frac{e^t}{t}\,dt$ is the exponential integral function [44, eq. (8.211.1)].

B. BAWT

Defining

$$\mathbf{D}_b(\Delta_f) = \mathrm{diag}\{e^{j2\pi\Delta_f}, e^{j4\pi\Delta_f}, \cdots, e^{j2\pi(N+1)\Delta_f}\},$$

then we can rewrite (10) as

$$\mathbf{r}_b = \mathbf{D}_b(\Delta_f)\mathbf{H}_l\mathbf{s} + \mathbf{D}_b(\Delta_f)\mathbf{F}_u\mathbf{s} + \mathbf{w}_b, \tag{14}$$

where

$$\mathbf{H}_l = \left[\begin{array}{c}\mathbf{H}\\ \mathbf{0}_{N,1}^T\end{array}\right], \quad \mathbf{F}_u = \left[\begin{array}{c}\mathbf{0}_{N,1}^T\\ \mathbf{F}\end{array}\right], \tag{15}$$

and $\mathbf{0}_{N,1}$ is a vector with N zero elements.

Subsequently, we can further have

$$\mathbf{r}_b = \mathbf{D}_b(\Delta_f)\boldsymbol{\Xi}\mathbf{s} + \mathbf{w}_b, \tag{16}$$

where

$$\boldsymbol{\Xi} = \mathbf{H}_l + \mathbf{F}_u. \tag{17}$$

With CSI at the receiver side, the capacity of (16) is

$$\begin{aligned} C_b =& \frac{1}{N+1}\mathrm{E}\left\{\log\det(\mathbf{I} + \gamma\mathbf{D}_\mathrm{b}(\Delta_\mathrm{f})\boldsymbol{\Xi}\boldsymbol{\Xi}^\mathrm{H}\mathbf{D}_\mathrm{b}^\mathrm{H}(\Delta_\mathrm{f}))\right\} \\ =& \frac{1}{N+1}E\{\log\det(\mathbf{I} + \gamma\boldsymbol{\Xi}\boldsymbol{\Xi}^H)\}, \end{aligned} \tag{18}$$

where $\boldsymbol{\Xi}\boldsymbol{\Xi}^H$ can be computed as a tridiagonal matrix (19), shown at the top of the next page.

Theorem 1. *Denote the upper bound and lower bound of C_b (18) by C_b^{up} and C_b^{low}, respectively. Then, there are*

$$\begin{aligned} C_b^{up} =& \frac{1}{N+1}\Bigg[(N-1)\log(1+\gamma\sigma_h^2+\gamma\sigma_f^2)) \\ & -\exp\left(\frac{1}{\gamma\sigma_h^2}\right)Ei\left(-\frac{1}{\gamma\sigma_h^2}\right) - \exp\left(\frac{1}{\gamma\sigma_f^2}\right)Ei\left(-\frac{1}{\gamma\sigma_f^2}\right)\Bigg], \end{aligned} \tag{20}$$

$$\begin{aligned} C_b^{low} =& \frac{1}{N+1}\Bigg[\log(2) + \frac{1}{2}\log(\sigma_h^2) + \frac{N+1}{2}\big(\log(\gamma) - Q\big) \\ & + \frac{N}{2}\log(\sigma_f^2) - \frac{N-1}{2}\exp\left(\frac{1}{\gamma\sigma_h^2}\right)Ei\left(-\frac{1}{\gamma\sigma_h^2}\right)\Bigg], \end{aligned} \tag{21}$$

where $Q \approx 0.5772$ is Euler's constant [44, eq. (9.73)].

Proof: See Appendix A. ∎

The channel capacity C_b under BAWT scheme is always larger than C_d under DWT one when

$$N \geq \left\lceil \frac{3C_d - C_1 - \log(4\sigma_h^2)}{-C_d + C_1 + \log(\sigma_f^2)} \right\rceil \text{ if } \log\left(\frac{\gamma\sigma_f^2}{1+\gamma\sigma_h^2}\right) > Q, \tag{22}$$

where $C_1 \triangleq \log(\gamma) - Q$.

Proof: Following by Jensen's inequality, there is

$$\mathrm{E}\left\{\log(1+\gamma|\mathrm{h(n)}|^2)\right\} \leq \log(1+\gamma\sigma_\mathrm{h}^2). \tag{23}$$

Together with (23), substituting (13) and (21) into $C_b^{\mathrm{low}} - C_d \geq 0$ gives the result (22). ∎

This article has been accepted for publication in a future issue of this journal, but has not been fully edited. Content may change prior to final publication. Citation information: DOI 10.1109/JSAC.2020.3005494, IEEE Journal on Selected Areas in Communications

$$\mathbf{\Xi}\mathbf{\Xi}^H = \begin{bmatrix} |h(1)|^2 & h(1)f^*(1) & 0 & \cdots & 0 & 0 & 0 \\ h^*(1)f(1) & |h(2)|^2+|f(1)|^2 & h(2)f^*(2) & \cdots & 0 & 0 & 0 \\ \vdots & \vdots & \vdots & \ddots & \vdots & \vdots & \vdots \\ 0 & 0 & 0 & \cdots & h^*(N-1)f(N-1) & |h(N)|^2+|f(N-1)|^2 & h(N)f^*(N) \\ 0 & 0 & 0 & \cdots & 0 & h^*(N)f(N) & |f(N)|^2 \end{bmatrix} \tag{19}$$

IV. Transceiver Design for DWT

A. Joint CFO and Channel Estimation

Motivated by the BEM

$$\mathbf{h} = \mathbf{B}_h\boldsymbol{\lambda}_h + \mathbf{e}_h, \tag{24}$$

we can further have

$$\mathbf{r}_d = \mathbf{D}_d(\Delta_f)\mathbf{S}\mathbf{B}_h\boldsymbol{\lambda}_h + \mathbf{D}_d(\Delta_f)\mathbf{S}\mathbf{e}_h + \mathbf{w}_d. \tag{25}$$

Here, $\boldsymbol{\lambda}_h = [\lambda_1, \lambda_2, \cdots, \lambda_M]^T$ is the vector consisting of the BEM coefficients, and $\mathbf{B}_h$ is an $N \times M$ matrix.

Selecting N_p rows from the basis matrix $\mathbf{B}_h$ as a new matrix $\mathbf{B}_{h,p} = \mathbf{B}_h([p_1, p_2, \cdots, p_{N_p}], :)$, the received signals corresponding to the N_p training symbols can be obtained as

$$\mathbf{r}_{d,p} = \mathbf{D}_{d,p}(\Delta_f)\mathbf{S}_p\mathbf{B}_{h,p}\boldsymbol{\lambda}_h + \mathbf{D}_{d,p}(\Delta_f)\mathbf{S}_p\mathbf{e}_{h,p} + \mathbf{w}_{d,p}, \tag{26}$$

where $\mathbf{S}_p = \text{diag}\{s(p_1), s(p_2), \cdots, s(p_{N_p})\}$, $\mathbf{w}_{d,p} = [w(p_1), w(p_2), \cdots, w(p_{N_P})]^T$, and $\mathbf{D}_{d,p}(\Delta_f) = \text{diag}\{e^{j2\pi p_1\Delta_f}, e^{j2\pi p_2\Delta_f}, \cdots, e^{j2\pi p_{N_p}\Delta_f}\}$.

Defining

$$\mathbf{G} = \mathbf{D}_{d,p}(\Delta_f)\mathbf{S}_p\mathbf{B}_{h,p}, \tag{27}$$

we can obtain the estimate of the BEM coefficients as

$$\hat{\boldsymbol{\lambda}}_h = (\mathbf{G}^H\mathbf{G})^{-1}\mathbf{G}^H\mathbf{r}_{d,p}. \tag{28}$$

Substitute (28) into (26), and then CFO Δ_f can be estimated by minimizing the square error

$$\widehat{\Delta}_f = \min_{\Delta_f} \|\mathbf{r}_{d,p} - \underbrace{\mathbf{G}(\mathbf{G}^H\mathbf{G})^{-1}\mathbf{G}^H}_{\mathbf{P}_G}\mathbf{r}_{d,p}\|^2, \tag{29}$$

where $\mathbf{P}_G$ is defined as the corresponding item. Noting that $(\mathbf{I}-\mathbf{P}_G)^H(\mathbf{I}-\mathbf{P}_G) = (\mathbf{I}-\mathbf{P}_G)$. Thus, we can further simplify (29) as

$$\begin{aligned} \widehat{\Delta}_f &= \min_{\Delta_f} \left((\mathbf{I}-\mathbf{P}_G)\mathbf{r}_{d,p}\right)^H (\mathbf{I}-\mathbf{P}_G)\mathbf{r}_{d,p} \\ &= \min_{\Delta_f} \left(\mathbf{r}_{d,p}^H\mathbf{r}_{d,p} - \mathbf{r}_{d,p}^H\mathbf{P}_G\mathbf{r}_{d,p}\right). \end{aligned} \tag{30}$$

Finally, we can obtain

$$\widehat{\Delta}_f = \max_{\Delta_f} \mathbf{r}_{d,p}^H\mathbf{P}_G\mathbf{r}_{d,p}, \tag{31}$$

which indicates that one dimensional search can estimate the CFO.

In summary, the receiver first estimates the CFO from (31) and the BEM coefficients from (28), and next recovers the time-varying channel as

$$\hat{\mathbf{h}} = \mathbf{B}_h\hat{\boldsymbol{\lambda}}_h. \tag{32}$$

B. Signal Detection

To recover the information symbols $s(n), n \in \mathcal{T}_d$, the receiver will calculate

$$\hat{s}(n) = \min_{s(n)} \|r_d(n) - e^{j2\pi n\widehat{\Delta}_f}\hat{h}(n)s(n)\|^2. \tag{33}$$

V. Transceiver Design for BAWT

A. Time-varying Channels $\mathbf{f}_0$ and $\mathbf{f}$

To facilitate estimation process, we give the following Proposition 1 and Theorem 2 for the direct channels $f_0(n)$ between the antenna of the BS and the antenna of the train, and the backscattered channels $f(n)$ between the antenna of the BS and the antenna of the mobile user.

Proposition 1. *The direct channels $f_0(n)$ at one fixed point of the rail in a static environment is not time-varying. It is the different locations of the receiver due to the train speed that result in the time selectivity of the channels $f_0(n)$.*

Proof: See Appendix B. ■

Trains run on preset rails and one train passes the same rail many times. Suppose at one fixed location, the train passed it at time n_1 and n_2. According to Proposition 1, we can claim that the channels $f_0(n_1)$ and $f_0(n_2)$ between the antenna of the BS and the outside antenna of the train are correlated if the broadcasting environment is unchanged at this location.

Define the time-varying channels $f_0(n)$ in one slot as

$$\mathbf{f}_0 = [f_0(1), f_0(2), \cdots, f_0(N)]^T. \tag{34}$$

According to (9), we can have

$$\mathbf{f} = \alpha\eta g_0 e^{-j2\pi f_{cs}} e^{j\Delta_\theta}\mathbf{f}_0. \tag{35}$$

Suppose the BEM for the channel vector $\mathbf{f}$ is

$$\mathbf{f} = \mathbf{B}_f\boldsymbol{\lambda}_f + \mathbf{e}_f, \tag{36}$$

where $\boldsymbol{\lambda}_f = [\lambda_1, \lambda_2, \cdots, \lambda_M]^T$ is the coefficient vector, $\mathbf{B}_f$ is the basis matrix, and $\mathbf{e}_f$ denotes the approximation error.

Assume the correlation matrix of the channel $\mathbf{f}_0$ is $\mathbf{R}_{f0} = \text{E}\{\mathbf{f}_0\mathbf{f}_0^{\text{H}}\}$ and its eigenvector decomposition is

$$\mathbf{R}_{f0} = \boldsymbol{\Phi}\boldsymbol{\Omega}\boldsymbol{\Phi}^H \tag{37}$$

where

$$\begin{aligned} \boldsymbol{\Phi} &= [\boldsymbol{\phi}_1, \boldsymbol{\phi}_2, \cdots, \boldsymbol{\phi}_N], \\ \boldsymbol{\Omega} &= \text{diag}\{\varpi_1, \varpi_2, \cdots, \varpi_N\}, \end{aligned}$$

$\varpi_1, \varpi_2, \cdots, \varpi_N$ are the eigenvalues of $\mathbf{R}_{f0}$ in a descending order, and $\boldsymbol{\phi}_1, \boldsymbol{\phi}_2, \cdots, \boldsymbol{\phi}_N$ are the corresponding eigenvectors.

This article has been accepted for publication in a future issue of this journal, but has not been fully edited. Content may change prior to final publication. Citation information: DOI 10.1109/JSAC.2020.3005494, IEEE Journal on Selected Areas in Communications

Theorem 2. *The lower bounds for the mean square error of* $\mathbf{e}_f$ *is*

$$\mathrm{E}\{\mathbf{e}_{\mathrm{f}}^{\mathrm{H}}\mathbf{e}_{\mathrm{f}}\} \geq \alpha^2\eta^2\sigma_{\mathrm{g0}}^2 \sum_{\mathrm{k=M+1}}^{\mathrm{N}} \varpi_{\mathrm{k}}. \tag{38}$$

and the corresponding optimal basis matrix for the time-varying channels $\mathbf{f}$ *is*

$$\mathbf{B}_f^{opt} = [\boldsymbol{\phi}_1, \boldsymbol{\phi}_2, \cdots, \boldsymbol{\phi}_M]. \tag{39}$$

Proof: See Appendix C. ■

Remark 2. *To obtain the real channel correlation matrix for the channel* $\mathbf{h}$ *is not practical since the mobile user can be in many places inside the train. However, it is possible to evaluate the channel correlation matrix* $\mathbf{R}_{f0}$ *for the channel* $\mathbf{f}_0$ *due to the fixed antenna on the top of the train.*

B. Joint CFO and Channel Estimation

We can rewrite (10) as

$$\mathbf{r}_b = \mathbf{D}_b(\Delta_f)\mathbf{S}_l\mathbf{h} + \mathbf{D}_b(\Delta_f)\mathbf{S}_u\mathbf{f} + \mathbf{w}_b, \tag{40}$$

where

$$\mathbf{S}_l = \begin{bmatrix} \mathbf{S} \\ \mathbf{0}_{N,1}^T \end{bmatrix} \quad \text{and} \quad \mathbf{S}_u = \begin{bmatrix} \mathbf{0}_{N,1}^T \\ \mathbf{S} \end{bmatrix}. \tag{41}$$

Substituting (24) and (36) into (40) will generate

$$\mathbf{r}_b = \mathbf{D}_b(\Delta_f)\mathbf{S}_l\mathbf{B}_h\boldsymbol{\lambda}_h + \mathbf{D}_b(\Delta_f)\mathbf{S}_u\mathbf{B}_f\boldsymbol{\lambda}_f + \mathbf{e} + \mathbf{w}_b, \tag{42}$$

where $\mathbf{e} = \mathbf{D}_b(\Delta_f)\mathbf{S}_l\boldsymbol{e}_h + \mathbf{D}_b(\Delta_f)\mathbf{S}_u\boldsymbol{e}_f$.

We can further obtain

$$\mathbf{r}_b = \mathbf{D}_b(\Delta_f)\mathbf{G}_{hf}[\boldsymbol{\lambda}_h^T, \boldsymbol{\lambda}_f^T]^T + \mathbf{e} + \mathbf{w}_b,$$

where $\mathbf{G}_{hf} = [\mathbf{S}_l\mathbf{B}_h \;\; \mathbf{S}_u\mathbf{B}_f]$. Next we can employ the similar joint estimator in Section IV-A to acquire the three estimates $\widehat{\Delta}_f$, $\hat{\boldsymbol{\lambda}}_h$, and $\hat{\boldsymbol{\lambda}}_f$.

Noting that the channels $\mathbf{f}$ are stronger than $\mathbf{h}$ due to the amplification factor α and no penetration loss. Accordingly, the signals from the backscatter path have more power than those from the direct path. We can thus motivate successive interference cancellation method to refine our estimates. That is, after estimating $\boldsymbol{\lambda}_f$, we can subtract the signals of the backscattered path from the received signals so as to better estimate $\boldsymbol{\lambda}_h$.

For brevity of our discussion, we assume that the first N_p symbols in each slot are training symbols. Define

$$\begin{aligned} \mathbf{r}_{b,p,h} &= [r_b(p_1), r_b(p_2), \cdots, r_b(p_{N_p})]^T, \\ \mathbf{r}_{b,p,f} &= [r_b(p_1+1), r_b(p_2+1), \cdots, r_b(p_{N_p}+1)]^T, \\ \mathbf{t}_f^{(1)} &= [r_b(p_1+1), r_b(p_2+1), \cdots, r_b(p_{N_p}+1)]^T. \end{aligned} \tag{43}$$

Selecting N_p rows from the basis matrix $\mathbf{B}_f$ as a new matrix

$$\mathbf{B}_{f,p} = \mathbf{B}_f([p_1+1, p_2+1, \cdots, p_{N_p}+1], :), \tag{44}$$

the initial estimate of the coefficient vector $\boldsymbol{\lambda}_f$ is

$$\hat{\boldsymbol{\lambda}}_f^{(1)} = e^{-j2\pi\Delta_f}(\mathbf{S}_p\mathbf{B}_{f,p})^{\dagger}\mathbf{D}_{d,p}(-\Delta_f)\mathbf{t}_f^{(1)}. \tag{45}$$

Next select the first $N_p - 1$ elements of the vector $\mathbf{t}_f^{(1)}$, and we can calculate $\mathbf{t}_h^{(1)}$ as

$$\mathbf{t}_h^{(1)} = \mathbf{r}_{b,p,h} - [0; \mathbf{t}_f^{(1)}(1:(N_p-1))]. \tag{46}$$

Then $\boldsymbol{\lambda}_h$ can be estimated as

$$\boldsymbol{\lambda}_h^{(1)} = (\mathbf{S}_p\mathbf{B}_{h,p})^{\dagger}\mathbf{D}_{d,p}(-\Delta_f)\mathbf{t}_h^{(1)}. \tag{47}$$

Now the CFO, the third estimate in this iteration, can be acquired as

$$\widehat{\Delta}_f^{(1)} = \min_{\Delta_f} \|\mathbf{t}_h^{(1)} - \mathbf{D}_{d,p}(\Delta_f)\mathbf{S}_p\mathbf{B}_{h,p}\boldsymbol{\lambda}_h^{(1)}\|^2. \tag{48}$$

Further, we can update $\mathbf{t}_h^{(1)}$ as

$$\mathbf{t}_h^{(2)} = \mathbf{D}_p(\widehat{\Delta}_f^{(1)})\mathbf{S}_p\mathbf{B}_{h,p}\hat{\boldsymbol{\lambda}}_h^{(1)}, \tag{49}$$

select its last $N_p - 1$ elements to construct a new vector $\mathbf{t}_h^{(2)}(2:N_p)$ and update $\mathbf{t}_f^{(1)}$ as

$$\mathbf{t}_f^{(2)} = \mathbf{r}_{b,p,f} - [\mathbf{t}_h^{(2)}(2:N_p); 0]. \tag{50}$$

Then iteratively repeat the steps from (45) to (50) until the following convergence condition is satisfied

$$|\widehat{\Delta}_f^{(n)} - \widehat{\Delta}_f^{(n-1)}| \leq \epsilon \tag{51}$$

where n indicates nth iteration and ϵ is a pre-set small constant.

Finally, the time-varying channels can be recovered at the last step as

$$\hat{\mathbf{h}} = \mathbf{B}_h\hat{\boldsymbol{\lambda}}_h^{(n)}, \quad \hat{\mathbf{f}} = \mathbf{B}_f\hat{\boldsymbol{\lambda}}_f^{(n)}. \tag{52}$$

C. Signal Detection

In this subsection, we propose three detectors to recover the data information $s(n), n \in \mathcal{T}_d$.

1) Maximum Likelihood (ML) Detector: The optimal detector will be ML detector

$$\hat{\mathbf{s}} = \arg\min_{\mathbf{s}} \|\mathbf{r}_b - \mathbf{D}_b(\widehat{\Delta}_f)\hat{\boldsymbol{\Xi}}\mathbf{s}\|^2, \tag{53}$$

where $\hat{\boldsymbol{\Xi}}$ is the estimated channel matrix constructed from $\hat{\mathbf{h}}$ and $\hat{\mathbf{f}}$. However, the ML detector has exponential complexity.

2) Successive Interference Cancelation (SIC) Detector: If low computational complexity is required, we can choose SIC decoding. The core idea of SIC is to decode signals associated with the largest channel gain first and then decode the remaining signals one by one by subtracting all decoded signals. Noting that the backscattered links $f(n)$ have more power than the direct links $h(n)$ due to less fading and the amplification factor α, we can recover $s(N)$ from the last symbol $r_b(N+1)$ first, and then recover $s(N-1)$ after subtracting $h(N)\hat{s}(N)$ from $r_b(N)$. Next, iteratively repeat the process and recover all $s(n)$. The data symbol $s(k)$ will thus be recovered as

$$\begin{aligned} \hat{s}(k) = \arg\min_{s(k)} \| & e^{-j2(k+1)\pi\widehat{\Delta}_f} r_b(k+1) \\ & - h(k+1)\hat{s}(k+1) - f(k)s(k)\|^2. \end{aligned} \tag{54}$$

This article has been accepted for publication in a future issue of this journal, but has not been fully edited. Content may change prior to final publication. Citation information: DOI 10.1109/JSAC.2020.3005494, IEEE Journal on Selected Areas in Communications

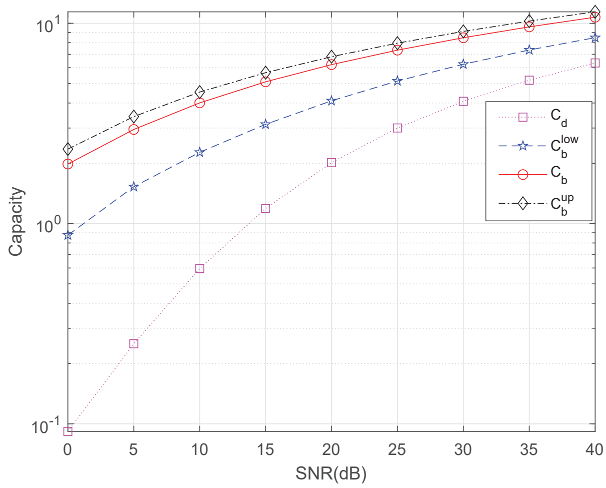

Fig. 4. Capacity versus SNR.

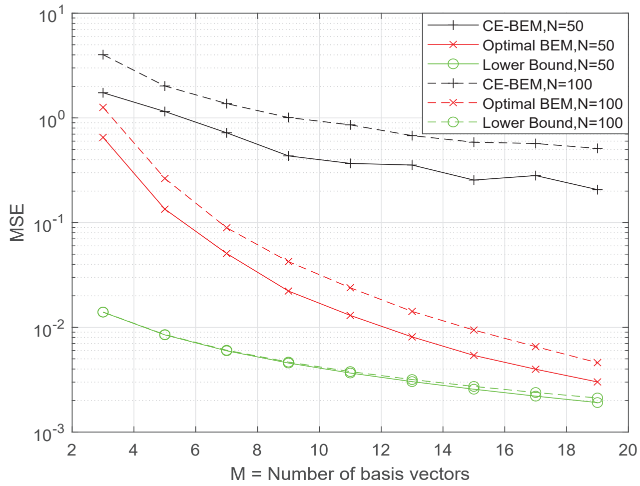

Fig. 6. MSE versus M.

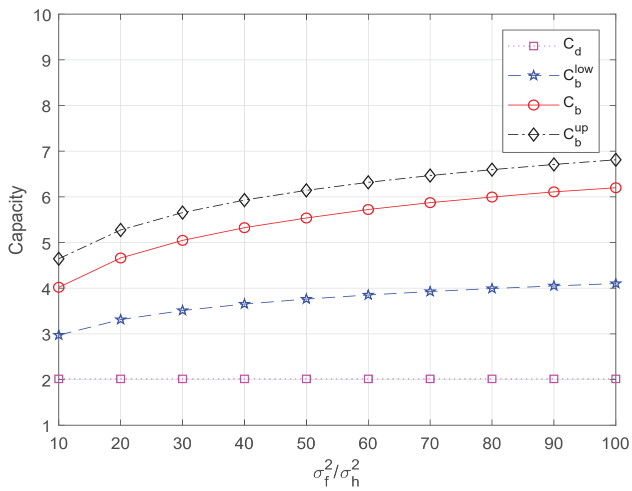

Fig. 5. Capacity versus σ_f^2/σ_h^2 when $\gamma = 20\,dB$.

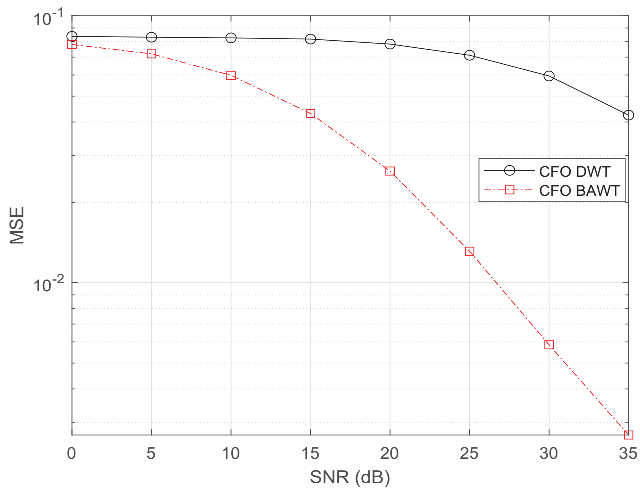

Fig. 7. MSE of Δ_f versus SNR.

3) Zero Forcing Detector: Multiply $\mathbf{r}_b$ with $\mathbf{D}_b(-\widehat{\Delta}_f)$ and $(\hat{\boldsymbol{\Xi}}^H\hat{\boldsymbol{\Xi}})^{-1}\hat{\boldsymbol{\Xi}}^H$ will obtain

$$\bar{\mathbf{r}}_b = (\hat{\boldsymbol{\Xi}}^H\hat{\boldsymbol{\Xi}})^{-1}\hat{\boldsymbol{\Xi}}^H\mathbf{D}_b(-\widehat{\Delta}_f)\mathbf{r}_b. \tag{55}$$

Then we can find that $\mathbf{s}$ has one-to-one correspondence with $\bar{\mathbf{r}}_b$. Accordingly, the data symbol $s(k)$ can be detected as

$$\hat{s}(k) = \arg\min_{s(k)} \|\bar{r}_b(k) - s(k)\|^2, \quad 1 \le k \le N \tag{56}$$

where $\bar{r}_b(k)$ denotes the kth symbol of $\bar{\mathbf{r}}_b$.

VI. Simulation Results

This section provides numerical examples to evaluate the proposed schemes. A key performance measure is the mean square error (MSE), which is defined as $\mathrm{MSE}(\hat{x}) = E\{(x-\hat{x})^2\}$ where $\hat{x}$ is the predicted value of the unknown parameter x. The second measure is the bit error ratio (BER), which is the number of incorrectly received bits divided by the total number of transferred bits. Some parameters are set as $\sigma_h^2 = 0.1$, $\sigma_f^2 = 10$ and $N = 50$, unless otherwise specified. The correlation matrix $\mathbf{R}_f$ of the channels $f(n)$ is modeled as $\mathbf{R}_f(m,n) = e^{-\frac{\rho|m-n|}{N}}$, where ρ is a positive real number that decides the relation tensity, and we take $\rho = 0.5$ in this section.

Fig. 4 and Fig. 5 respectively illustrate channel capacity versus SNR and the ratio σ_f^2/σ_h^2. It can be found that the upper bound and lower bound of channel capacity are close to the exact channel capacity. Importantly, the BAWT scheme achieves higher rates with increasing channel variance σ_f^2 compared with the DWT scheme.

Fig. 6 plots the approximate MSE of our suggested BEM. For comparison, the MSE of the complex exponential basis expansion model (CE-BEM) [46] is also provided. Fig. 6 shows that our suggested BEM outperforms the CE-BEM, all MSE reduces and approaches the lower bounds (38) as the number of basis vectors increases.

Fig. 7 depicts the MSE of Δ_f versus SNR, and Fig. 8 shows the MSE of $\boldsymbol{h}$ and $\boldsymbol{f}$ versus SNR in the case of estimate and exact value of Δ_f, respectively. As seen in Fig. 7 and Fig. 8, MSEs of all estimates drop with increasing SNR. Moreover, the estimation accuracies of all estimates in the BAWT case are better than the counterparts in the DWT scheme.

Fig. 9 shows the BER curves of the three detectors of our

This article has been accepted for publication in a future issue of this journal, but has not been fully edited. Content may change prior to final publication. Citation information: DOI 10.1109/JSAC.2020.3005494, IEEE Journal on Selected Areas in Communications

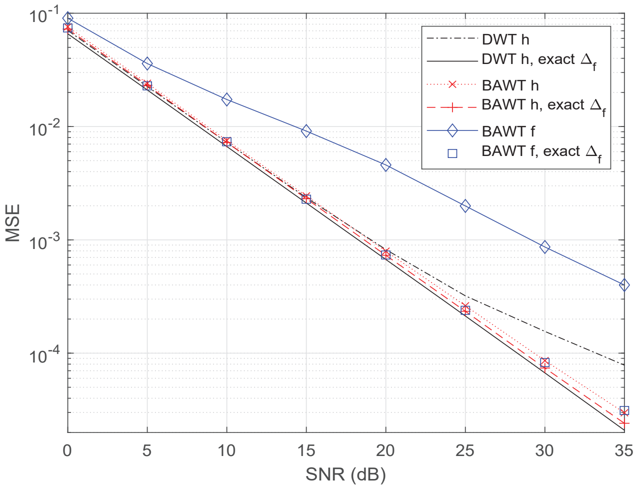

Fig. 8. MSE of $\boldsymbol{h}$ and $\boldsymbol{f}$ versus SNR.

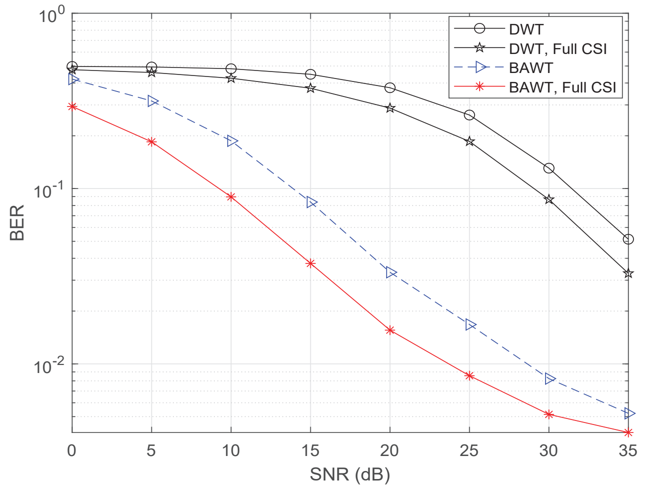

Fig. 10. BER versus SNR.

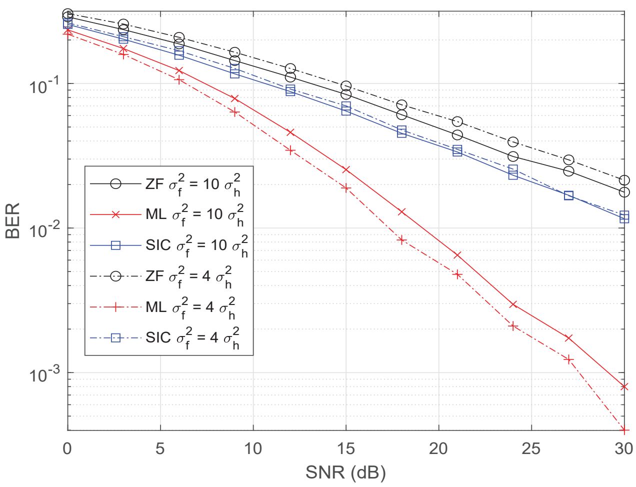

Fig. 9. BER performance of three detectors with perfect channel state information.

proposed BAWT scheme: ML, SIC, and ZF with perfectly known channel parameters at the receivers. We set $N = 10$ and plot BER curves for both cases: $\sigma_f^2 = 4\sigma_h^2$ and $\sigma_f^2 = 10\sigma_h^2$. It can be seen from Fig. 9 that ML detector is optimal, and ZF detector outperforms SIC detector. It is also worth noting that ML has the optimal performance, and also the highest time complexity which is exponential.

Fig. 10 exhibits the detection BER versus SNR after the estimates Δ_f, $\boldsymbol{h}$ and $\boldsymbol{f}$ are obtained and when perfect parameters Δ_f, $\boldsymbol{h}$ and $\boldsymbol{f}$ are assumed. As seen, the BER curve of BAWT scheme is exactly below the DWT one, which implies that BAWT outperforms DWT in detection.

VII. Conclusion

In this paper, we introduced backscatter technology into HSR wireless communication systems in order to reduce the signal penetration loss and to facilitate channel estimation. We showed that our proposed BAWT scheme can reduce complexity and achieve low cost compared with traditional solutions such as relaying and beamforming. We also suggested and compared BAWT and DWT transmission schemes, including the joint CFO channel estimator and the signal detector. We demonstrated that BAWT could outperform DWT in capacity, estimation and detection. To our best knowledge, our work is the first study about backscatter aided HSR wireless communications. We conclude on the positive note that there are many, related open problems for future research, including training sequence design, joint estimation and detection, and channel encoding.

Appendix A
Proof of Theorem 1

Define $C_b' = (N+1)C_b$. Then, we have

$$\begin{aligned} C_b' =& E\{\log|\mathbf{I} + \gamma \boldsymbol{\Xi}\boldsymbol{\Xi}^H|\} \\ \overset{(a)}{\leq}& E\{\log(1+\gamma h^2(1))\} + E\{\log(1+\gamma f^2(N))\} \\ &+ \sum_{n=2}^{N} E\{\log(1+\gamma h^2(n) + \gamma f^2(n-1))\} \\ \overset{(b)}{\leq}& E\{\log(1+\gamma h^2(1))\} + E\{\log(1+\gamma f^2(N))\} \\ &+ \sum_{n=2}^{N} \log(1+\gamma E\{h^2(n) + f^2(n-1)\}), \end{aligned} \tag{57}$$

where (a) and (b) follow by Fischer's inequality and Jensen's inequality, respectively. Suppose the upper bound (57) of C_b' is denoted by $C_b^{\mathrm{up}'}$, which can be computed as

$$\begin{aligned} C_b^{\mathrm{up}'} =& (N-1)\log(1+\gamma\sigma_h^2 + \gamma\sigma_f^2) - \exp\left(\frac{1}{\gamma\sigma_h^2}\right)\times \\ & \mathrm{Ei}\left(-\frac{1}{\gamma\sigma_h^2}\right) - \exp\left(\frac{1}{\gamma\sigma_f^2}\right)\mathrm{Ei}\left(-\frac{1}{\gamma\sigma_f^2}\right). \end{aligned} \tag{58}$$

Let us separately set $\boldsymbol{M}_D$ and $\boldsymbol{M}_U$ as (59) and (60), shown

$$\boldsymbol{M}_D = \begin{bmatrix} \gamma|h(1)|^2 & 0 & 0 & \cdots & 0 & 0 & 0 \\ \gamma h^*(1)f(1) & 1+\gamma|h(2)|^2 & 0 & \cdots & 0 & 0 & 0 \\ \vdots & \vdots & \vdots & \ddots & \vdots & \vdots & \vdots \\ 0 & 0 & 0 & \cdots & \gamma h^*(N-1)f(N-1) & 1+\gamma|h(N)|^2 & 0 \\ 0 & 0 & 0 & \cdots & 0 & \gamma h^*(N)f(N) & 1 \end{bmatrix} \tag{59}$$

$$\boldsymbol{M}_U = \begin{bmatrix} 1 & \gamma h(1)f^*(1) & 0 & \cdots & 0 & 0 & 0 \\ 0 & \gamma|f(1)|^2 & 0 & \cdots & 0 & 0 & 0 \\ \vdots & \vdots & \vdots & \ddots & \vdots & \vdots & \vdots \\ 0 & 0 & 0 & \cdots & 0 & \gamma|f(N-1)|^2 & \gamma h(N)f^*(N) \\ 0 & 0 & 0 & \cdots & 0 & 0 & \gamma|f(N)|^2 \end{bmatrix} \tag{60}$$

at the top of next page. Subsequently, there is

$$\begin{aligned} C_b' =& E\{\log\det(\boldsymbol{M}_D+\boldsymbol{M}_U)\} \\ \overset{(c)}{\geq}& E\{\log(\det(\boldsymbol{M}_D)+\det(\boldsymbol{M}_U))\} \\ \overset{(d)}{\geq}& E\left\{\log\left(2\sqrt{\det(\boldsymbol{M}_D)\det(\boldsymbol{M}_U)}\right)\right\}, \end{aligned} \tag{61}$$

where (c) follows by $\det(\boldsymbol{A}_{M,M}+\boldsymbol{B}_{M,M}) \geq \det(\boldsymbol{A}_{M,M}) + \det(\boldsymbol{B}_{M,M})$ with both $\boldsymbol{A}$ and $\boldsymbol{B}$ positive semidefinite matrix, and (d) follows by $a+b \geq 2\sqrt{ab}$. Denote the lower bound (61) of C_b' by $C_b^{\text{low}'}$. Then, with the help of [44, eq. (4.331.1)], eq. (61) can be further calculated as

$$\begin{aligned} C_b^{\text{low}'} =& \frac{1}{2}\log(\sigma_h^2) + \frac{N}{2}\log(\sigma_f^2) + \frac{N+1}{2}\left(\log(\gamma)-Q\right) \\ &+ \log(2) - \frac{N-1}{2}\exp\left(\frac{1}{\gamma\sigma_h^2}\right)\text{Ei}\left(-\frac{1}{\gamma\sigma_h^2}\right). \end{aligned} \tag{62}$$

Therefore, separately substituting (58) and (62) into

$$C_b^{\text{low}} = \frac{1}{N+1}C_b^{\text{low}'} \tag{63}$$

and

$$C_b^{\text{up}} = \frac{1}{N+1}C_b^{\text{up}'}, \tag{64}$$

the upper bound C_b^{up} and lower bound C_b^{low} can be derived.

Appendix B
Proof of Proposition 1

Consider a sinusoidal signal $e^{j2\pi f_{cs}n+\theta_s}$ is transmitted and M copies are received at one terminal due to multiple paths, as depicted in Fig. 11. The receiver moves towards the transmitter at a speed of v m/s.

The received signal can be expressed as

$$r(n) = \sum_{m=0}^{M} L_m^{-\alpha/2} e^{j(2\pi f_{cs}n+\theta_s-\frac{2\pi(L_m-vn\cos(\beta_m))}{\lambda})}, \tag{65}$$

where L_m represents each path length at the time $n=0$, α is the path loss component with typical values as 2 or 3. It is worth noting that $v\cos(\beta_m)/\lambda$ in (65) is the Doppler shift of the mth path.

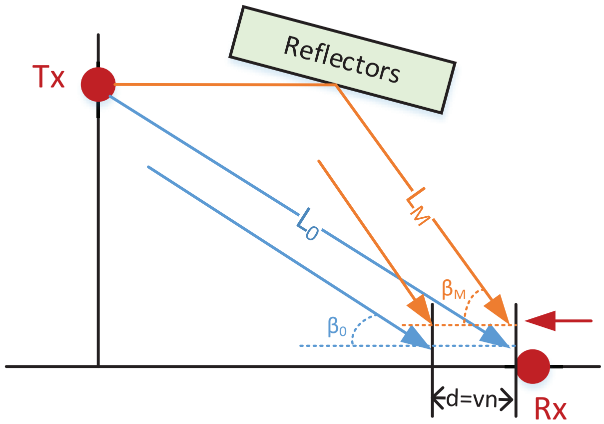

Fig. 11. Various train speed results in different locations of the receiver.

Define $d=vn$, and we can rewrite (65) as

$$r(n) = \sum_{m=0}^{M} L_m^{-\alpha/2} e^{j2\pi f_{cs}n} e^{j\theta_s} e^{j(-\frac{2\pi L_m}{\lambda})} e^{j(\frac{2\pi d\cos(\beta_m)}{\lambda})}. \tag{66}$$

Accordingly, the channel $f_0(n)$ in such single carrier case can be considered as

$$f_0(n) = \sum_{m=0}^{M} L_m^{-\alpha/2} e^{-j\frac{2\pi L_m}{\lambda}} e^{j\frac{2\pi d\cos(\beta_m)}{\lambda}}. \tag{67}$$

It can be readily checked from (67) that when the environment around HSR is static, given the location d, the channel $f_0(n)$ is fixed even when the receiver are moving. The moving speed v only decides the length of d, i.e., different locations of the receiver.

Appendix C
Proof of Theorem 2

Substituting the least square estimate $\hat{\boldsymbol{\lambda}}_f = (\mathbf{B}_f^H\mathbf{B}_f)^{-1}\mathbf{B}_f^H\mathbf{f}$ into $\text{E}\{\mathbf{e}_\text{f}^\text{H}\mathbf{e}_\text{f}\}$ will produce

$$\begin{aligned} \text{E}\{\mathbf{e}_\text{f}^\text{H}\mathbf{e}_\text{f}\} =& \text{E}\|\mathbf{f}-\mathbf{B}_\text{f}\boldsymbol{\lambda}_\text{f}\|^2 \\ =& \text{E}\|(\mathbf{I}-\mathbf{B}_\text{f}(\mathbf{B}_\text{f}^\text{H}\mathbf{B}_\text{f})^{-1}\mathbf{B}_\text{f}^\text{H})\mathbf{f}\|^2. \end{aligned} \tag{68}$$

This article has been accepted for publication in a future issue of this journal, but has not been fully edited. Content may change prior to final publication. Citation information: DOI 10.1109/JSAC.2020.3005494, IEEE Journal on Selected Areas in Communications

There exists an orthonormal matrix

$$\mathbf{B} = [\underbrace{\mathbf{b}_1, \mathbf{b}_2, \cdots, \mathbf{b}_M}_{\mathbf{B}_f}, \mathbf{b}_{M+1}, \cdots, \mathbf{b}_N], \tag{69}$$

where $\mathbf{B}_f$ is defined as the corresponding item.

It can be readily obtained that

$$\mathbf{I} - \mathbf{B}_f(\mathbf{B}_f^H\mathbf{B}_f)^{-1}\mathbf{B}_f^H = \mathbf{B}\mathbf{I}_{1,N-M}^{0,M}\mathbf{B}^H, \tag{70}$$

where $\mathbf{I}_{1,N-M}^{0,M}$ is a diagonal matrix with M zeroes and $N-M$ ones on the diagonal

$$\mathbf{I}_{1,N-M}^{0,M} = \mathrm{diag}\{\underbrace{0, 0, \cdots, 0}_{M}, \underbrace{1, 1, \cdots, 1}_{N-M}\}. \tag{71}$$

Subsequently, we can simplify (68) as

$$\begin{aligned} \mathrm{E}\{\mathbf{e}_\mathrm{f}^\mathrm{H}\mathbf{e}_\mathrm{f}\} &= \mathrm{E}\{\mathbf{f}^\mathrm{H}\mathbf{B}\mathbf{I}_{1,\mathrm{N-M}}^{0,\mathrm{M}}\mathbf{B}^\mathrm{H}\mathbf{B}\mathbf{I}_{1,\mathrm{N-M}}^{0,\mathrm{M}}\mathbf{B}^\mathrm{H}\mathbf{f}\} \\ &= \mathrm{E}\{\mathrm{tr}\{\mathbf{I}_{1,\mathrm{N-M}}^{0,\mathrm{M}}\mathbf{B}^\mathrm{H}\mathbf{f}\mathbf{f}^\mathrm{H}\mathbf{B}\}\}. \end{aligned} \tag{72}$$

Noting that

$$\mathrm{E}\{\mathbf{f}\mathbf{f}^\mathrm{H}\} = \alpha^2\eta^2\sigma_{g_0}^2\mathrm{E}\{\mathbf{f}_0\mathbf{f}_0^\mathrm{H}\} = \alpha^2\eta^2\sigma_{\mathrm{g}_0}^2\mathbf{R}_{\mathrm{f}0}. \tag{73}$$

Therefore, we can have

$$\mathrm{E}\{\mathbf{e}_\mathrm{f}^\mathrm{H}\mathbf{e}_\mathrm{f}\} = \mathrm{tr}\{\alpha^2\eta^2\sigma_{\mathrm{g}_0}^2\mathbf{I}_{1,\mathrm{N-M}}^{0,\mathrm{M}}\mathbf{B}^\mathrm{H}\mathbf{R}_{\mathrm{f}0}\mathbf{B}\}. \tag{74}$$

In the case of $\mathbf{B} = \mathbf{\Phi}$, i.e., setting $\mathbf{B}$ as the eigenvector matrix of $\mathbf{R}_{f0}$, we can obtain

$$\mathrm{E}\{\mathbf{e}_\mathrm{f}^\mathrm{H}\mathbf{e}_\mathrm{f}\} \geq \alpha^2\eta^2\sigma_{\mathrm{g}_0}^2\mathrm{tr}\{\mathbf{I}_{1,\mathrm{N-M}}^{0,\mathrm{M}}\mathbf{\Omega}\} = \alpha^2\eta^2\sigma_{\mathrm{g}_0}^2\sum_{\mathrm{k=M+1}}^{\mathrm{N}}\varpi_\mathrm{k}.$$

REFERENCES

[1] B. Ai, X. Cheng, T. Kürner, Z. Zhong, K. Guan *et al.*, "Challenges toward wireless communications for high-speed railway," *IEEE Trans. Intelligent Transportation Systems*, vol. 15, no. 5, pp. 2143-2158, Oct. 2014.

[2] W. Zhou, J. Wu, and P. Fan, "High mobility wireless communications with Doppler diversity: Fundamental performance limits," *IEEE Trans. Wireless Commun.*, vol. 14, no. 12, pp. 6981-6992, Dec. 2015.

[3] R. He, C. Schneider, B. Ai, G. Wang, D. Dupleich *et al.*, "Propagation channels of 5G millimeter wave vehicle-to-vehicle communications: recent advances and future challenges," *IEEE Veh. Technol. Mag.*, vol. 15, no. 1, pp.16-26, Mar. 2019.

[4] R. He, B. Ai, G. L. Stber, G. Wang and Z. Zhong, "Geometrical-based modeling for millimeter-Wave MIMO mobile-to-mobile channels," *IEEE Trans. Veh. Technol.*, vol. 67, no. 4, pp. 2848-2863, Apr. 2018.

[5] Z. Zhang, X. Chai, K. Long, Athanasios V. Vasilakos and L. Hanzo, "Full-duplex techniques for 5G networks: self-interference cancellation, protocol design and relay selection", *IEEE Commun. Mag.*, vol. 53, no. 5, pp. 128-137, May 2015.

[6] G. Wang, Q. Liu, R. He, F. Gao and C. Tellambura, "Acquisition of channel state information in heterogeneous cloud radio access networks: challenges and research directions," *IEEE Wireless Commun.*, vol. 22, no. 3, pp. 100-107, Jun. 2015.

[7] T. Li, X. Wang, P. Fan and T. Riihonen, "Position-aided large-scale MIMO channel estimation for high-speed railway communication systems," *IEEE Trans. Veh. Technol.*, vol. 66, no. 10, pp. 8964-8978, Oct. 2017.

[8] L. H. Yang, G. L. Ren, Z. Qiu, "A novel doppler frequency offset estimation method for DVB-T system in HST environment", *IEEE Trans. Broadcast.*, vol. 58, no. 1, pp. 139-143, Jun. 2012.

[9] O. Karimi, J. Liu, C. Wang, "Seamless wireless connectivity for multimedia services in high-speed trains", *IEEE J. Sel. Areas Commun.*, vol. 30, no. 5, pp. 729-739, May 2012.

[10] J. You, Z. Zhong, Z. Dou, J. Dang, and G. Wang, "Wireless relay communication on high-speed railway: full duplex or half duplex?", *China Commun.*, vol. 13, no. 11, pp. 14-26, Nov. 2016.

[11] X. Kang, C. K. Ho and S. Sun, "Full-duplex wireless-powered communication network with energy causality," *IEEE Trans. Wireless Commun.*, vol. 14, no. 10, pp. 5539-5551, Oct. 2015.

[12] S. Zhang, F. Gao, H. Wang and C. Pei, "Dynamic individual channel estimation for one-way Relay networks with time-multiplexed-superimposed training," *IEEE Trans. Veh. Technol.*, vol. 63, no. 8, pp. 3841-3852, Oct. 2014.

[13] X. Xie, M. Peng, F. Gao and W. Wang, "Superimposed training based channel estimation for uplink multiple access relay networks," *IEEE Trans. Wireless Commun.*, vol. 14, no. 8, pp. 4439-4453, Aug. 2015.

[14] S. Zhang, F. Gao, J. Li and M. Sheng, "Online and offline Bayesian Cramér-Rao bounds for time-varying channel estimation in one-way relay networks," *IEEE Trans. Signal Process.*, vol. 63, no. 8, pp. 1977-1992, Apr. 2015.

[15] G. Wang, F. Gao, W. Chen and C. Tellambura, "Channel estimation and training design for two-way relay networks in time-selective fading environments," *IEEE Trans. Wireless Commun.*, vol. 10, no. 8, pp. 2681-2691, Aug. 2011.

[16] Y. Ge, W. Zhang, F. Gao, S. Zhang and X. Ma, "Beamforming network optimization for reducing channel time variation in high-mobility massive MIMO," *IEEE Transa. Commun.*, vol. 67, no. 10, pp. 6781-6795, Oct. 2019.

[17] C. Xing, Y. Jing, S. Wang, S. Ma and H. V. Poor, "New viewpoint and algorithms for water-filling solutions in wireless communications," *IEEE Trans. Signal Processing*, vol. 68, pp. 1618-1634, Feb. 2020.

[18] W. Guo, W. Zhang, P. Mu and F. Gao, "High-mobility OFDM downlink transmission with large-scale antenna array," *IEEE Trans. Veh. Technol.*, vol. 66, no. 9, pp. 8600-8604, Sep. 2017.

[19] Y. Ge, W. Zhang, F. Gao and H. Minn, "Angle-domain approach for parameter estimation in high-mobility OFDM with fully/partly calibrated massive ULA," *IEEE Trans. Wireless Commun.*, vol. 18, no. 1, pp. 591-607, Jan. 2019.

[20] Z. Li, F. Zhou, X. Chen, Y. Li and F. Gao, "An adaptive state assignment mechanism based on joint data detection and channel estimation on fading meteor channel," *IEEE Trans. Veh. Technol.*, vol. 66, no. 6, pp. 4627-4635, Jun. 2017.

[21] J. Li, S. Yan, Y. Liu, B. M. Hochwald and J. Jin, "A high-order model for fast estimation of electromagnetic absorption induced by multiple transmitters in portable devices," *IEEE Trans. Antennas and Propag.*, vol. 65, no. 12, pp. 6768-6778, Dec. 2017.

[22] J. D. Griffin and G. D. Durgin, "Gains for RF tags using multiple antennas," *IEEE Trans. Antennas Propag.*, vol. 56, no. 2, pp. 563-570, Feb. 2008.

[23] C. Boyer and S. Roy, "Backscatter communication and RFID: coding, energy and MIMO analysis," *IEEE Trans. Commun.*, vol. 62, no.3, pp. 770-785, Mar. 2014.

[24] H. Stockman, "Communication by means of reflected power," in *Proc. IRE*, pp.1196-1204, Oct. 1948.

[25] W. Zhao, G. Wang, S. U. B. Atapattu, R. He and Y. Liang, "Channel estimation for ambient backscatter communication systems with massive-antenna reader," *IEEE Trans. Veh. Technol.*, vol. 68, no. 8, pp. 8254-8258, Aug. 2019.

[26] Q. Tao, C. Zhong, H. Lin and Z. Zhang, "Symbol detection of ambient backscatter systems with manchester coding," *IEEE Trans. Wireless Commun.*, vol. 17, no. 6, pp. 4028-4038, Jun. 2018.

[27] J. Kimionis, A. Bletsas, and J. N. Sahalos, "Increased range bistatic scatter radio," *IEEE Trans. Commun.*, vol. 62, no. 3, pp. 1091-1104, Mar. 2014.

[28] V. Liu, A. Parks, V. Talla, S. Gollakota, D. Wetherall, and J. R. Smith, "Ambient backscatter: wireless communication out of thin air," in *ACM SIGCOMM*, Hong Kong, China, 2013, pp. 1-13.

[29] W. Zhao, G. Wang, S. Atapattu, T. A. Tsiftsis, and X. Ma, "Performance analysis of large intelligent surface aided backscatter communication systems," accepted by *IEEE Wireless Commun. Letters*, Feb. 2020. DOI: 10.1109/LWC.2020.2976934.

[30] W. Zhao, G. Wang, S. Atapattu, T. A. Tsiftsis, and C. Tellambura, "Is backscatter link stronger than direct link in reconfigurable intelligent surface-assisted system?," accepted by *IEEE Commun. Letters*, Feb. 2020. DOI: 10.1109/LCOMM.2020.2980510.

[31] B. Kellogg, A. Parks, S. Gollakota, J. R. Smith, and D. Wetherall, "Wi-Fi backscatter: Internet connectivity for RF-powered devices," in *ACM SIGCOMM*, Chicago, USA, 2014, pp. 1-12.

[32] S. Ma, G. Wang, R. Fan, and C. Tellambura, "Blind channel estimation for ambient backscatter communication systems," *IEEE Commun. Lett.*, vol. 22, no. 6, pp. 1296-1299, Jun. 2018.

[33] G. Wang, F. Gao, R. Fan, and C. Tellambura, "Ambient backscatter communication systems: detection and performance analysis," *IEEE Trans. Commun.*, vol.64, no.11, pp. 4836-4846, Nov. 2016.

[34] N. Van Huynh, D. T. Hoang, X. Lu, D. Niyato, P. Wang and D. I. Kim, "Ambient backscatter communications: a contemporary survey," *IEEE Commun. Surveys & Tutorials*, vol. 20, no. 4, pp. 2889-2922, Fourthquarter 2018.

[35] X. Kang, Y. Liang and J. Yang, "Riding on the Primary: A New Spectrum Sharing Paradigm for Wireless-Powered IoT Devices," *IEEE Trans. Wireless Commun.*, vol. 17, no. 9, pp. 6335-6347, Sept. 2018.

[36] S. Zhang, F. Gao, J. Li and H. Li, "Time varying channel estimation for dstc-based relay networks: tracking, smoothing and BCRBs," *IEEE Trans. Wireless Commun.*, vol. 14, no. 9, pp. 5022-5037, Sep. 2015.

[37] Y. Yang, F. Gao, X. Ma and S. Zhang, "Deep learning-based channel estimation for doubly selective fading channels," *IEEE Access*, vol. 7, pp. 36579-36589, Mar. 2019.

[38] X. Ma, G. B. Giannakis, and S. Ohno, "Optimal training for block transmissions over doubly selective wireless fading channels," *IEEE Trans. Signal Process.*, vol. 41, no. 5, pp. 1351-1366, May 2003.

[39] M. Dong, L. Tong, and B. Sadler, "Optimal insertion of pilot symbols for transmissions over time-varying flat fading channels," *IEEE Trans. Signal Process.*, vol. 52, no. 5, pp. 1403-1418, May 2004.

[40] M. Li, S. Zhang, N. Zhao, W. Zhang and X. Wang, "Time-Varying massive MIMO channel estimation: capturing, reconstruction, and restoration," *IEEE Trans. Commun.*, vol. 67, no. 11, pp. 7558-7572, Nov. 2019.

[41] J. Ma, S. Zhang, H. Li, F. Gao and S. Jin, "Sparse Bayesian learning for the time-varying massive MIMO channels: acquisition and tracking," *IEEE Trans. Commun.*, vol. 67, no. 3, pp. 1925-1938, Mar. 2019.

[42] H. Xie, F. Gao, S. Zhang and S. Jin, "A unified transmission strategy for TDD/FDD massive MIMO systems with spatial basis expansion model," *IEEE Trans. Veh. Technol.*, vol. 66, no. 4, pp. 3170-3184, Apr. 2017.

[43] M. K. Simon, *Probability distributions involving Gaussian random variables: a handbook for engineers and scientists*. Springer, 2006.

[44] I. S. Gradshteyn and I. M. Ryzhik, *Table of integrals, series and products* , 7th ed. Academic Press Inc, 2007.

[45] M. Dong and L. Tong, "Optimal design and placement of pilot symbols for channel estimation," *IEEE Trans. Signal Process.*, vol. 50, no. 12, pp. 3055-3069, Dec. 2002.

[46] C. W. R. Chiong, Y. Rong and Y. Xiang, "Channel estimation for time-varying MIMO relay systems," *IEEE Trans. Wireless Commun.*, vol. 14, no. 12, pp. 6752-6762, Dec. 2015.

Wenjing Zhao received the B.Eng. degree in computer science and technology from Beijing Jiaotong University, Beijing, China, in 2016. She is currently pursuing the Ph.D. degree with the Department of Computer Science and Technology, Beijing Jiaotong University, Beijing, China. Her research interests include Internet of Things, performance analysis theories, and signal processing technologies.

Gongpu Wang received the B.Eng. degree from Anhui University, Hefei, Anhui, China, in 2001, and the M.Sc. degree from Beijing University of Posts and Telecommunications, Beijing, China, in 2004. From 2004 to 2007, he was an assistant professor in School of Network Education, Beijing University of Posts and Telecommunications. He received Ph.D. degree from University of Alberta, Edmonton, Canada, in 2011. Currently, he is a professor in School of Computer and Information Technology, Beijing Jiaotong University, China. His research interests include wireless communication theories, signal processing technologies, and Internet of Things.

Bo Ai (M'00SM'10) received the M.S. and Ph.D. degrees from Xidian University, Xian, China, in 2002 and 2004, respectively. He was with Tsinghua University, Beijing, China, where he was an Excellent Post-Doctoral Research Fellow in 2007. He is currently a Professor and a Doctoral Supervisor with the Beijing Jiaotong University. He is also the Deputy Director of the State Key Laboratory of Rail Traffic Control and Safety. He has published six Chinese academic books, three English books, over 110 IEEE journal articles, five ESI highly cited papers, and one ESI hot paper. He has obtained nine international conference paper awards and 26 invention patents: 18 proposals adopted by the ITU, 3GPP, and so on and eight provincial and ministerial-level science and technology awards. He is mainly engaged in the research and application of the theory and core technology of broadband mobile communication and rail transit dedicated mobile communication systems (GSM-R, LTE-R, 5G-R, and LTE-M).

Dr. Ai is the IET Fellow. He received the National Science Fund for Distinguished Young Scholars, the Outstanding Youth Science Fund, the Ministry of Science and Technologys Young and Middle-aged Science and Technology Innovation Leaders, the China Association for Science and Technologys Seeking Outstanding Youth Award, the Ministry of Educations New Century Excellence Talent, Zhan Tianyou Railway Science and Technology Youth Award, Beijing Science and Technology Star Winner, and the Honorary Title of Beijing Excellent Teacher. He is also the President of the IEEE BTS Xian Branch, the Vice President of the IEEE VTS Beijing Branch, the IEEE VTS Distinguished Lecturer, an Associate Editor of the IEEE TRANSACTIONS ON CONSUMER ELECTRONICS and the IEEE TRANSACTIONS ON ANTENNAS AND PROPAGATION, the Guest Editor of the IEEE ANTENNAS AND WIRELESS PROPAGATION LETTERS, the IEEE TRANSACTIONS ON VEHICULAR TECHNOLOGY, the IEEE TRANSACTIONS ON INDUSTRIAL ELECTRONICS, and other SCI journals.

Jian Li (M'17) received the B.S., M.S., and Ph.D. degrees in communication and information system from the University of Electronic Science and Technology of China, Chengdu, China, in 2007, 2010, and 2015, respectively. He was a Visiting Scholar with the Center for Computational Electromagnetics, Department of Electrical and Computer Engineering, University of Illinois at UrbanaChampaign, Urbana, IL, USA, from 2015 to 2016. He is currently an Associate Professor with the University of Electronic Science and Technology of China. He has authored or co-authored over 30 papers in refereed journals and conferences. His current research interests include bioelectromagnetics, applied electromagnetics, and RF, microwave, millimeterwave integrated circuits and system, and electromagnetic metamaterials and its applications.

Chintha Tellambura (F'11) received the B.Sc. degree in electronics and telecommunications from the University of Moratuwa, Sri Lanka, the M.Sc. degree in electronics from the Kings College, University of London, and the Ph.D. degree in electrical engineering from the University of Victoria, Canada. He was with Monash University, Australia, from 1997 to 2002. Since 2002, he has been with the Department of Electrical and Computer Engineering, University of Alberta, where he is currently a Full Professor. He has authored or coauthored over 560 journal and conference papers, with an h-index of 74 (Google Scholar). He has supervised or co-supervised 66 M.Sc., Ph.D., and PDF trainees. His current research interests include cognitive radio, heterogeneous cellular networks, fifth-generation wireless networks, and machine learning algorithms. He was elected as a fellow of The Canadian Academy of Engineering in 2017. He received the Best Paper Awards from the IEEE International Conference on Communications (ICC) in 2012 and 2017. He is the winner of the prestigious McCalla Professorship and the Killam Annual Professorship from the University of Alberta. He served as an Editor for the IEEE TRANSACTIONS ON COMMUNICATIONS from 1999 to 2012 and IEEE TRANSACTIONS ON WIRELESS COMMUNICATIONS from 2001 to 2007. He was an Area Editor of Wireless Communications Systems and Theory from 2007 to 2012.